THEORETICAL MODELS FOR COOPERATIVE STEADY-STATE ATPASE ACTIVITY OF MYOSIN SUBFRAGMENT-1 ON REGULATED ACTIN

TERRELL L. HILL, EVAN EISENBERG, AND J. M. CHALOVICH, *Laboratory of Molecular Biology, National Institute of Arthritis, Metabolism, and Digestive Diseases; Laboratory of Cell Biology, National Heart and Lung Institute, National Institutes of Health, Bethesda, Maryland 20205 U.S.A.*

ABSTRACT Recent theoretical work on the cooperative equilibrium binding of myosin subfragment-1-ADP to regulated actin, as influenced by Ca^{2+}, is extended here to the cooperative steady-state ATPase activity of myosin subfragment-1 on regulated actin. Exact solution of the general steady-state problem will require Monte Carlo calculations. Three interrelated special cases are discussed in some detail and sample computer (not Monte Carlo) solutions are given. The eventual objective is to apply these considerations to in vitro experimental data and to in vivo muscle models.

INTRODUCTION

In a recent paper (1), we introduced a theoretical model (Appendix) for the cooperative equilibrium binding of S-1 (myosin subfragment-1) to regulated actin (i.e., to the actin-troponin-tropomyosin complex), in the presence and in the absence of Ca^{2+}. The model was applied to the experimental data of Greene and Eisenberg (2). Here we show how the theory can be extended to the cooperative, in vitro, steady-state ATPase activity of S-1 on regulated actin.

This is a paper on theoretical methodology. To present the theory, we adopt illustrative numerical parameter choices that are more or less plausible and that were suggested in part by our preliminary experimental work. However, the actual application of the model to our own data, with new parameters, requires more experimental work and will be the subject of a future publication. In the meantime, we hope that the model and methods might prove useful to other experimental groups that have done or are doing (3–5) experimental work of the same general type.

Although the model mentioned above could be treated exactly when applied to the equilibrium binding of S-1 and Ca^{2+} (1), there is no hope of doing this, with complete generality, for the much more difficult steady-state problem of interest in the present paper without resorting to Monte Carlo calculations (6, 7). We plan to use Monte Carlo calculations in the future, but for the present we make use of approximations or of assumptions about rate constants that allow explicit numerical solutions.

The present problem serves as a rather complicated one-dimensional example of systems of interacting enzyme molecules in the steady state. We have given the theoretical treatment of such systems considerable attention in recent years (6–13).

The obvious next step in our theoretical program will be to attempt to extend the

considerations to be outlined here to the in vivo steady-state (and transient) interaction of actin and myosin filaments as influenced by Ca^{2+} (i.e., to the regulation of muscle contraction by Ca^{2+}). The formalism (14–16) we have been using in our work on muscle models (17–19) already includes possible variations in the concentrations of ATP, ADP, and P_i, but it does not include Ca^{2+} effects.

We have recently begun to consider a second, alternative model[1,2] for our cooperative equilibrium binding studies. We shall not use this model here but we expect to test it, along with the present model, in the analysis of our ATPase data. The second model assumes that tropomyosin-troponin has only one stable position in the actin groove, rather than two. However, this single stable position is shifted to a varying extent in the presence of Ca^{2+} or of the S-1-nucleotide complex bound to actin. Therefore this model allows more flexibility in the interpretation of nucleotide effects. Monte Carlo calculations will be needed for the cooperative ATPase problem, using this model, except in the special case of section 1.

1. ATPASE ACTIVITY AT ARBITRARY ACTIN CONCENTRATION AND VERY DILUTE S-1

In this and the following two sections, we discuss three "different" ATPase models, all based on the same equilibrium binding model (1). Actually, the three models are logically related to each other and overlap in ways that will be explained below. The first two models correspond to experiments that are relatively easy to carry out. The basic rate constants used are the same in the three models; the differences in the models are related to different experiments or approximations.

We employ the general kinetic model for the actomyosin ATPase reviewed in reference 20. But, for simplicity, we use here a reduced three-state ATPase cycle

$$\begin{array}{ccc} R & \rightleftharpoons & N \\ & \nwarrow \quad \swarrow\!\!\!\swarrow & \\ & MD & \end{array} \qquad (1)$$

for S-1 unattached to actin. The five first-order rate constants are included in Fig. 1 (the units are s^{-1}, with c_A in μM). The notation (20) here is $R \equiv M \cdot D \cdot Pi_R$ and $N \equiv M \cdot D \cdot Pi_N$, where $M \equiv$ S-1, $D \equiv$ ADP, and R and N refer to two different conformations (refractory, nonrefractory). Other species in the complete ATPase cycle (20) are assumed here to be transient intermediates and are therefore omitted from the cycle. To include ATP concentration effects (3), we would have to include a fourth state (M) in the cycle. The reverse transition $R \rightarrow MD$ in Eq. 1 is omitted because the corresponding rate constant is virtually zero (to be consistent with the free energy of hydrolysis of ATP). The same three-state cycle is also used when S-1 is attached to actin (Fig. 1), but the rate constants are different. There would be no difficulty, except the addition of more rate constants, in increasing the number of states in the cycle beyond three.

---

[1]Hill, T. L. 1981. Binding under a molecular "umbrella" as a cooperative statistical mechanical system: tropomyosin-actin-myosin as an example. *Biophys. Chem.* (In press).

[2]Hill, T. L., E. Eisenberg, and L. Greene. Alternative model, including nucleotide effects, for the binding of myosin subfragment-1 to the actin-troponin-tropomyosin complex. Manuscript in preparation.

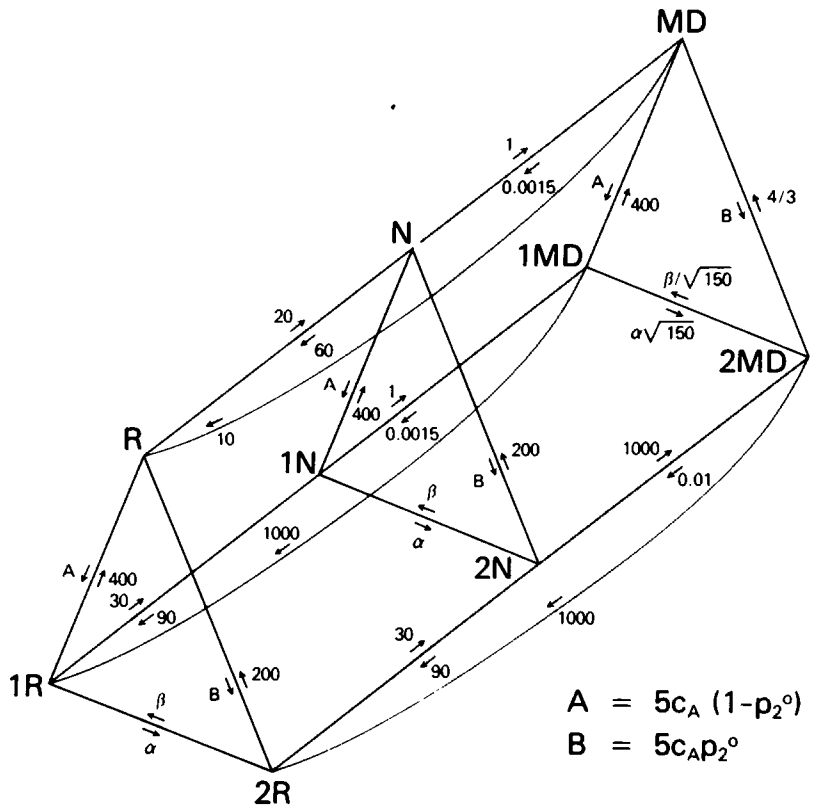

FIGURE 1 Kinetic diagram and first-order rate constants in s^{-1} for a single S-1 molecule when S-1 concentration is very low. A, B, α, and β depend on Ca^{2+} concentration via p_2^o. The tropomyosin unit to which the single S-1 may be attached is in state labeled 1 or 2. Rate constant assignments are merely illustrative. See text for further details.

As in the previous paper (1), and as summarized in the Appendix, we assume that each tropomyosin-troponin unit (including seven sites on the actin filament) can be in one of two possible conformations or states, referred to as 1 (weak) and 2 (strong). There are nearest-neighbor (pair) interactions between these units that depend on the states (1 or 2) of the two units and on the number of Ca^{2+} (0, 1, or 2) bound to the regulatory sites of the troponin that is nearer the overlap region of the pair in question (1). These pair interactions are assumed not to be influenced by the binding of R, N, or MD onto the actin sites of the two units of a pair. Also, it is assumed that these S-1 species do not interact with each other when bound on adjacent actin sites. Binding of Ca^{2+} to troponin is assumed to be relatively fast, and always at equilibrium. The notation $1R$, in Fig. 1, refers to one S-1 molecule in state R bound to any one of the seven actin sites of a unit in state 1.

In general, the six equilibrium binding constants for R, N, and MD onto state 1 or onto state 2 sites might all be different (but there are only three different binding constants in Fig. 1). The five rate constants in each of the two "attached" ATPase cycles are assumed here, for simplicity, to be uninfluenced by Ca^{2+} binding. But such effects can easily be included, if necessary.

The approach that we take in Fig. 1 is to follow the "life history" of one particular S-1 molecule, as it makes transitions among nine possible states. The S-1, when unattached to actin and in state R, N, or MD, can bind an actin monomer (or site) from an actin pool with free concentration c_A (in monomer units), and thus move to one of the six "attached" states in Fig. 1. Because the solution (in this model) is very dilute in S-1, c_A is essentially the same as the total actin concentration c_A^o. The actin sites or monomers belong to two classes: those in state 1 units (fraction $1 - p_2^o$) and those in state 2 units (fraction p_2^o). The superscript on p_2^o refers to the fact that this is the fraction of state 2 units in the virtual absence of S-1 (i.e., for "empty" actin); thus p_2^o is a cooperative equilibrium property that may be calculated from Eq. 12 of reference 1 (or Eq. 3 below) on putting c (free S-1 concentration) = 0. Fig. 1 allows for the binding of either type of actin site, with concentration $c_A(1 - p_2^o)$ or $c_A p_2^o$, onto R, N, or MD.

Binding of S-1 is assumed to be diffusion-controlled in Fig. 1. Hence A and B (at six places in the figure) include the same second-order rate constant, 5 s^{-1} μM^{-1}. Note the three different dissociation rate constants (400, 200, and 4/3 s^{-1}); hence there are three different equilibrium binding constants, with notation and values $K_1 = 5/400 = 0.0125$ μM^{-1}, $K_2' = 5/200 = 0.025$ μM^{-1}, $K_2 = 5/(4/3) = 3.75$ μM^{-1}, respectively. Note that $K_2' > K_1$ and $K_2 \gg K_1$.

The rate constants α and β refer to a change in state of the particular seven-site unit to which the one S-1 is attached (no other S-1 will be bound to this unit, or to neighboring units, because $c \to 0$). Detailed balance in any of the three triangles in Fig. 1 requires that

$$\alpha/\beta = 2S, \quad S \equiv p_2^o/(1 - p_2^o). \tag{2}$$

S is a property of "empty" regulated actin; the factor of two is the ratio K_2'/K_1 for S-1 binding. The extra factor of 150 in the MD triangle arises from the larger binding constant of MD to state 2; this equilibrium factor is "split" symmetrically between the two rate constants α and β (Fig. 1). This particular split is plausible but arbitrary. Detailed balance is also satisfied within each of the six rectangles of the diagram (Fig. 1).

The ATPase activity can be followed by means of the three essentially irreversible transitions $MD \to R$, $1MD \to 1R$, and $2MD \to 2R$ that complete the three ATPase cycles. The sum of the rates of the latter two transitions gives the actin-activated ATP flux.

Although Eq. 2 expresses the ratio α/β correctly in terms of p_2^o, the simple kinetics implied by the inverse rate constants α, β (at three places in Fig. 1) cannot be exact at steady state (except when $\alpha, \beta \to 0$; see section 3). The involvement of only a single seven-site unit in Fig. 1 amounts to a kind of "mean field" approximation. This follows because, for example, for the transition $2R \to 1R$, four different rate constants would in general be involved (rather than only one, β), depending on whether the two nearest-neighbor units of the primary unit are in states 11, 12, 21, or 22 (9). Furthermore, one cannot use equilibrium considerations (9) to determine the relative weights of these four rate constants (and thus calculate β as an average) because the steady-state activity within the diagram (Fig. 1) will lead to a state 2 to state 1 ratio for the attached states (e.g., $2R$ to $1R$) of the primary unit that does not correspond to equilibrium for any one of R, N, or MD. This, in turn, will result in probabilities of states 11, 12, 21, and 22 for the two nearest-neighbor units of the primary unit that deviate from equilibrium values.

To summarize: for this case, $c \rightarrow 0$, there is cooperativity between states 1 and 2 in the empty regulated actin, but no further cooperativity is introduced by the minimal S-1 binding; however, each bound S-1 will perturb the state 1/state 2 distribution of empty units in its immediate neighborhood.

Explicit Introduction of Interactions and Ca^{2+}

We use here the model and notation of the previous paper (1). Details are given in the Appendix. The interaction parameters $Y_{ij}(\rho)$, for an ij pair of units ($i, j = 1, 2$), depend on the Ca^{2+} concentration ρ. The intrinsic equilibrium constant (1) favoring a state 1 unit over a state 2 unit, in the absence of S-1, Ca^{2+}, or neighbor interactions, is L. The explicit expression for $p_2^o(\rho)$ in Eq. 2 is (1)

$$p_2^o(\rho) = 2aY^{-1}/\sqrt{\quad}\,(1 - a + \sqrt{\quad})$$
$$\sqrt{\quad} \equiv [(1 - a)^2 + 4aY^{-1}]^{1/2} \tag{3}$$
$$Y \equiv Y_{11}(\rho)Y_{22}(\rho)/Y_{12}(\rho)Y_{21}(\rho)$$
$$a \equiv Y_{22}(\rho)/LY_{11}(\rho) \equiv 1/L'(\rho). \tag{4}$$

These equations refer to regulated actin in the absence of S-1 but at an arbitrary concentration ρ of Ca^{2+}.

Equilibrium binding studies (1) of *MD*, or other forms of S-1, on regulated actin can provide values of $Y(\rho)$ and $L'(\rho)$. According to the model we are using here, these parameters are properties of the regulated actin at ρ, but they should be independent of the form of bound S-1 used to determine them. From this point on, in the present paper, we shall confine ourselves to the limiting Ca^{2+} concentrations $\rho \rightarrow 0$ and $\rho \rightarrow \infty$, and assume that we have available, from binding studies, values of $Y(0)$, $Y(\infty)$, $L'(0)$ and $L'(\infty)$. Hence, we can calculate $p_2^o(0)$ and $p_2^o(\infty)$ from Eq. 3, and then $S(0)$ and $S(\infty)$ in Eq. 2.

In both of the relations (Eq. 2)

$$\alpha(0)/\beta(0) = 2S(0), \quad \alpha(\infty)/\beta(\infty) = 2S(\infty), \tag{5}$$

the "intrinsic" (see above) value of the α/β ratio is $1/L$. If we form the product

$$[\alpha(0)/\alpha(\infty)][\beta(\infty)/\beta(0)] = S(0)/S(\infty), \tag{6}$$

both L and the S-1 factor $K_2'/K_1 = 2$ cancel out, so that the right-hand side of Eq. 6 can be associated with Ca^{2+} and interaction effects alone. At this point we assume, as usual, that these effects are split symmetrically between α and β. That is, we assume

$$\alpha(0)/\alpha(\infty) = \beta(\infty)/\beta(0) = [S(0)/S(\infty)]^{1/2}. \tag{7}$$

Thus, if we assign a value to $\alpha(0)$, as an arbitrary reference rate constant, we can then calculate $\beta(0)$ from Eq. 5, $\alpha(\infty)$ from Eq. 7, and $\beta(\infty)$ from Eqs. 5 or 7. Because these four rate constants relate to a conformation or state change of the long tropomyosin complex, it seems reasonable to expect that their magnitudes are fairly small. But there is a practical limit to this: $\sqrt{150}\ \alpha(\infty)$ should not be less than the rate of activation of muscle tension and $\beta(0)$ should not be less than the rate of relaxation of tension. These rates are of order 10–20 s^{-1}. A value for the reference constant $\alpha(0)$ of 1 s^{-1} would not be too small (see below).

Numerical Calculations

As a numerical example, we take $L'(0) = 30$, $Y(0) = 5$, $L'(\infty) = 4$, $Y(\infty) = 1$. These values are based on preliminary binding experiments at low salt. They give (Eq. 3) $p_2^o(0) = 6.985 \times 10^{-3}$ and $p_2^o(\infty) = 0.20$. Thus, in the absence of Ca^{2+}, L' is larger (favoring state 1 more), and the cooperativity is stronger (1). Of course, with $c \to 0$, as in this section, the cooperativity is in the empty actin and is not noticeable in the flux (Fig. 2). To complete the set of rate constants in Fig. 1, we have to assign values of c_A and $\alpha(0)$ [from which we calculate $\alpha(\infty)$, $\beta(0)$, and $\beta(\infty)$]. Then, for each of the two Ca^{2+} cases $\rho = 0$ and $\rho = \infty$, which affect α, β, A, and B in Fig. 1, we solve (by computer) nine linear algebraic equations (16) in nine unknowns to find the steady-state probabilities (p_R, etc.) of the nine states in the kinetic diagram (Fig. 1). The total ATP flux (in s^{-1}) per S-1 molecule is then most easily found from (Fig. 1)

$$J = 10p_{MD} + 1{,}000(p_{1MD} + p_{2MD}). \tag{8}$$

The non-actin–activated flux ($10p_{MD}$) is usually negligible.

We have calculated curves $J(c_A)$, for $\rho = 0$ and $\rho = \infty$, choosing $\alpha(0) = 0.01$, 1.0, 10.0, and 100.0 s^{-1}. When $\alpha(0)$ is 1.0 s^{-1}, we find $\beta(0) = 71.1$, $\alpha(\infty) = 5.96$, and $\beta(\infty) = 11.92$ s^{-1}. These constants all vary proportionally when the value of $\alpha(0)$ is changed. Fig. 2 shows curves of $J(c_A)$ at $\rho = 0$ and $\rho = \infty$ and for $\alpha(0) = 0.01$, 10.0, and 100.0 s^{-1}. In the $\alpha(0) = 0.01$ s^{-1} case, the maximum values of $J(c_A \to \infty)$ are 1.05 s^{-1} for $\rho = 0$ and 14.5 s^{-1} for $\rho = \infty$. The separate points near the $\alpha(0) = 0.01$ s^{-1} curves are for the case $\alpha(0) = 1.0$ s^{-1}. The differences between $\alpha(0) = 0.01$ and 1.0 s^{-1} are small.

The problems posed in the next two sections are difficult to treat unless we assume $\alpha, \beta \to$

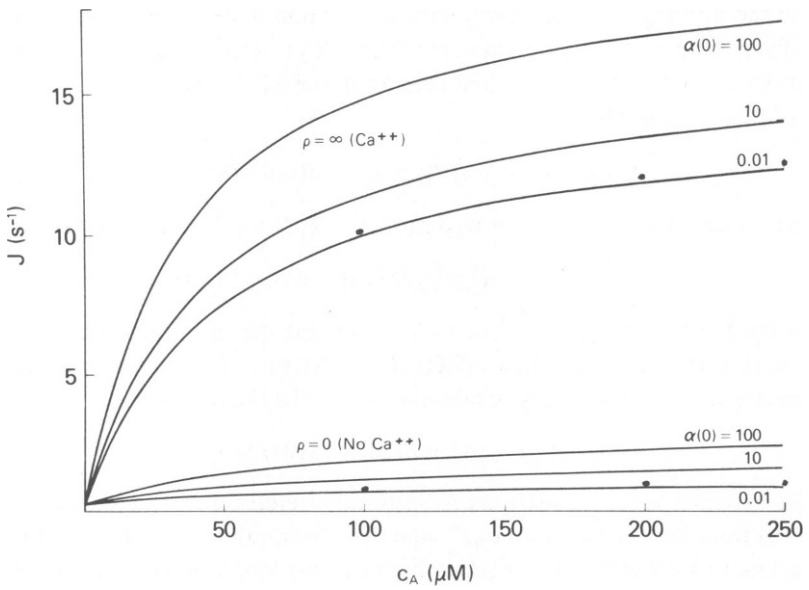

FIGURE 2 Calculated ATP flux J (per S-1) as function of actin monomer concentration c_A, at high Ca^{2+} ($\rho = \infty$) or low Ca^{2+} ($\rho = 0$), as calculated from the diagram in Fig. 1. Four choices are made for $\alpha(0)$, in s^{-1}. The six isolated points are for $\alpha(0) = 1$ s^{-1}. See text for further details.

0. In this section, the realistic choice $\alpha(0) = 1\ s^{-1}$ practically amounts to $\alpha, \beta \to 0$ (see above). This suggests but does not guarantee that the use of $\alpha, \beta \to 0$ in the next two sections may also be effectively consistent with observed rates of activation and relaxation of muscle tension.

2. ATPASE ACTIVITY AT ARBITRARY S-1 CONCENTRATION AND VERY DILUTE ACTIN

This case is the opposite of that in the preceding section. Because very little actin is present ($c_A^o \to 0$) virtually all of the S-1 is free, with concentration c, and, furthermore, the fractions p_R, p_N, and p_{MD} of subspecies R, N, and MD in this free S-1 pool can be calculated from Fig. 3*a* alone (i.e., the binding to actin hardly perturbs the steady-state pool).

It is natural in this case to consider the kinetic diagram of an actin site (Fig. 3 *b*) rather than of an S-1 molecule (as in Fig. 1). However, this diagram is unrealistic because the seven sites of a unit necessarily change state ($1 \rightleftharpoons 2$) together, and also it is necessary to take into account the possible states 11, 12, 21, and 22 of the two nearest neighbor units. In fact, a Monte Carlo treatment of a long linear array of seven-site units is required to handle this problem exactly.

However, if the units are assumed to change state slowly compared to the rates of the other transitions, then the problem becomes tractable and can be treated without further approximation. We make this assumption here; comments on its possible validity were made at the end of the preceding section.

We now approach the problem as indicated schematically in Fig. 3 *c*. Each of the seven sites of a unit, say in state 1, is able to achieve an independent steady state among the states 10, 1*R*, 1*N*, and 1*MD* (because $1 \to 2$ is slow). There is a particular rate constant $\alpha(n)$, for $1 \to 2$, associated with any distribution $n \equiv n_0, n_R, n_N, n_{MD}$ of the seven sites ($n_0 + n_R + n_N + n_{MD} =$

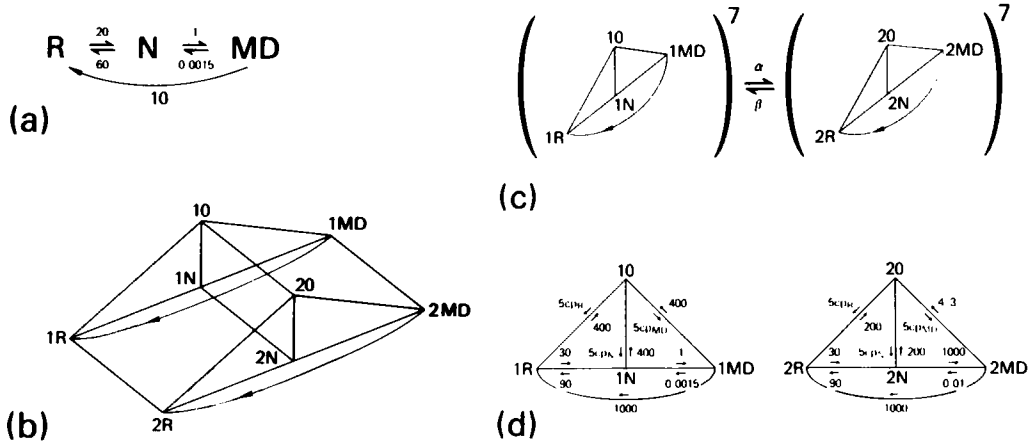

FIGURE 3. This case corresponds to very low actin concentration, but arbitrary S-1 concentration. (*a*) Kinetic diagram for an S-1 molecule in solution. (*b*) Kinetic diagram for a single actin site. 0 refers to an empty site. (*c*) Schematic treatment of a unit of seven actin sites when α and β are small. Each site of a unit in state 1 or in state 2 comes to an independent steady-state distribution within the diagrams shown in (*d*). See text for further details.

7) among the four states (0 refers to an empty site). Let $P_1(n)$ be the probability of such a distribution for a state 1 unit. Then α in Fig. 3 *c* is an average over all possible distributions:

$$\alpha = \sum_n \alpha(n)P_1(n), \quad \beta = \sum_n \beta(n)P_2(n). \tag{9}$$

The analogous expression for β is also given here. If α/β, an effective equilibrium constant, is calculated under the proper conditions (see below), nearest-neighbor interactions between units can also be included in the model without approximation. In essence, at steady state, because $1 \rightleftharpoons 2$ transitions are relatively slow, there is an equilibrium distribution between the two types of units, including interactions between neighboring units (an equilibrium Ising problem), while within each type of unit there is a steady-state distribution among the four states 0, *R*, *N*, and *MD* (determined from Fig. 3 *d*). This, incidentally, is just the reverse of the usual situation in biochemical kinetics (16, 21) in which we have a steady-state distribution among states, each of which is assumed to be in internal equilibrium.

To exploit this point of view explicitly, we begin with a closely related equilibrium problem. If the three irreversible transitions $MD \rightarrow R$ are omitted from Figs. 3 *a* and *c*, we have a three-state equilibrium binding system that is a generalization of the model treated in reference 1. The fraction of state 2 units (Eqs. 3 and 4) is

$$p_2 = 2aY^{-1}/\sqrt{\quad}\,(1 - a + \sqrt{\quad}), \tag{10}$$

a function of Y and a only. Here a is given by

$$a = (1 + 2K_2'c + K_2c)^7/L'(\rho)(1 + 3K_1c)^7. \tag{11}$$

The K's are the binding constants of S-1 introduced in the previous section. This generalization of Eq. 17 of reference 1 follows immediately from the properties of subsystem grand partition functions (22). The physical significance (1) of a is that this is the equilibrium constant, per tropomyosin unit, for the transition $1 \rightleftharpoons 2$ between a filament with all units in state 1 and a filament with all units in state 2.

In order to relate Eq. 11 to the steady-state problem, we now examine this equilibrium equation from a kinetic point of view. Because a is an equilibrium constant, we can also rewrite it formally as a rate constant quotient:

$$a = \alpha/\beta = (\alpha_o/\beta_o)(1 + 2K_2'c + K_2c)^7/(1 + 3K_1c)^7$$

$$\alpha_o/\beta_o = 1/L'(\rho). \tag{12}$$

Thus, α_o/β_o is the quotient in the absence of S-1 binding ($c = 0$, as in Eq. 4). We now show that Eq. 12 follows from Eq. 9. This will serve to check the validity of Eq. 9 and will also provide a framework for the analogous steady-state calculation.

For an arbitrary distribution n (see above),

$$\alpha(n) = \alpha_o(K_2'/K_1)^{f(n_R+n_N)}\,(K_2/K_1)^{fn_{MD}} \tag{13}$$

$$\beta(n) = \beta_o(K_1/K_2')^{(1-f)(n_R+n_N)}\,(K_1/K_2)^{(1-f)n_{MD}} \tag{14}$$

$$P_i(n) = 7!\,p_{i0}^{n_0}\,p_{iR}^{n_R}\,p_{iN}^{n_N}\,p_{iMD}^{n_{MD}}/n_0!n_R!n_N!n_{MD}! \qquad (i = 1, 2) \tag{15}$$

where f is the kinetic split factor (8) and the p's are equilibrium binding probabilities (22):

$$p_{10} = 1/(1 + 3K_1c), \quad p_{1R} = p_{1N} = p_{1MD} = K_1c/(1 + 3K_1c)$$
$$p_{20} = 1/(1 + 2K_2'c + K_2c), \quad p_{2R} = p_{2N} = K_2'c/(1 + 2K_2'c + K_2c)$$
$$p_{2MD} = K_2c/(1 + 2K_2'c + K_2c). \tag{16}$$

The justification of Eqs. 13 and 14 is as follows. The factors α_o and β_o are the rate constants in the absence of S-1 binding. Binding of a single R or N onto a unit alters the relative thermodynamic stability of state 2 compared to state 1 by a factor K_2'/K_1, and binding of an MD introduces a similar factor K_2/K_1. These binding free energy effects will also appear as correction factors in the rate constants, $(K_2'/K_1)^f$ in α and $(K_1/K_2')^{1-f}$ in β, etc. In the absence of other information, f might be taken as $f = \frac{1}{2}$ ("symmetrical split").

If we now substitute Eqs. 13–15 into Eq. 9, we obtain

$$\alpha = \alpha_o[p_{10} + (K_2'/K_1)^f(p_{1R} + p_{1N}) + (K_2/K_1)^f p_{1MD}]^7 \tag{17}$$

$$\beta = \beta_o[p_{20} + (K_1/K_2')^{1-f}(p_{2R} + p_{2N}) + (K_1/K_2)^{1-f}p_{2MD}]^7. \tag{18}$$

Finally, on introducing the equilibrium Eq. 16 into these expressions, we recover Eq. 12 (for arbitrary f), as was to be proved.

We turn now to the steady-state version of Eq. 12. Eqs. 9, 13, and 14 apply at steady state as well as at equilibrium. Eq. 15 also applies at steady state, as shown on page 153 of reference 16. Hence Eqs. 17 and 18 are again obtained, at steady state, but now the p's (two separately normalized sets) are to be found from the two independent steady-state diagrams in Fig. 3 *d*. In this figure, c is the total free S-1 concentration whereas p_R, p_N, and p_{MD} (pool fractions) follow from Fig. 3 *a* (in fact, $p_R = 0.735$, $p_N = 0.241$, $p_{MD} = 0.0241$). The two sets of p's from Fig. 3 *d* must be calculated (by computer) for each value of c. However, these sets are not dependent on the value of ρ.

From Eqs. 17 and 18, we now have, in place of Eq. 12,

$$a = \alpha/\beta = [1]^7/L'(\rho)[2]^7 \tag{19}$$

where the brackets, which depend on c but not on ρ, are those in Eqs. 17 and 18. In our calculations below we use $f = \frac{1}{2}$; also $K_2'/K_1 = 2$ and $K_2/K_1 = 300$ (see above). Thus, in summary, we have made use of a kinetic argument in order to generalize a in the equilibrium Eq. 11 to the steady-state case of interest here. This steady state a may be used in Eq. 10 to obtain p_2 because of the quasi-equilibrium nature of this model, as explained above.

Only the actin-activated ATP flux J_a (per actin monomer) is of interest here. This is given (in s^{-1}) by

$$J_a = 1{,}000[(1 - p_2)p_{1MD} + p_2p_{2MD}]. \tag{20}$$

Incidentally, the fraction of actin sites (either state) occupied by S-1 (in any form) is

$$\theta = (1 - p_2)(1 - p_{10}) + p_2(1 - p_{20}). \tag{21}$$

Numerical Calculations

Fig. 4 *a* shows J_a, p_2, and θ as functions of c for the $\rho = \infty$ case, whereas Fig. 4 *b* gives the same functions in the absence of Ca^{2+} ($\rho = 0$). The maximum value of J_a ($c \to \infty$), in both figures, is

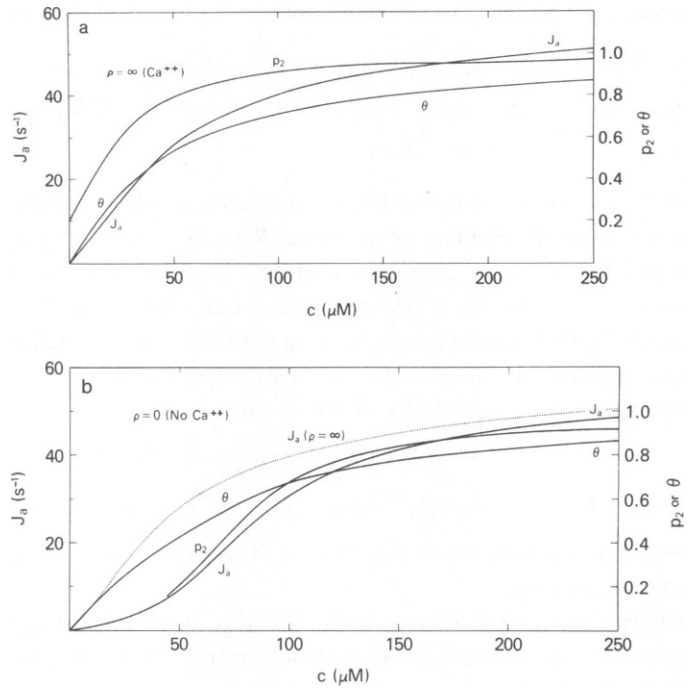

FIGURE 4 (*a*) Calculation of actin-activated flux J_a (per actin monomer) as function of S-1 concentration c at high Ca^{2+} and low actin concentration. See text. (*b*) Same as (*a*) except at low Ca^{2+} concentration. The dotted curve is from (*a*), for comparison. The fraction of occupied actin sites is θ; p_2 is the fraction of units in state 2. See text.

$J_a \cong 60\ s^{-1}$. Because of the much larger rate constant for $2N \rightarrow 2MD$ (1,000 s^{-1}) than for $1N \rightarrow 1MD$ (1 s^{-1}), J_a is strongly dependent on p_2. In Fig. 4 *a* ($\rho = \infty$), p_2 has a significant value (0.20) even at $c = 0$, whereas $p_2 = 0.007$ at $c = 0$ in Fig. 4 *b* ($\rho = 0$). These initial values of p_2 (i.e., p_2^o) are determined roughly (1) by $1/L'Y$. Most of the initial flux (near $c = 0$) in Fig. 4 *a* comes from $2MD$ whereas, because p_2 is so small, it comes from $1MD$ in Fig. 4 *b*. The p_2 curve falls on top of the J_a curve in Fig. 4 *b*, for $c < 50\ \mu M$. Appreciable flux in Fig. 4 *b* ($\rho = 0$) is delayed to larger values of c after state 2 and, in particular, $2MD$ achieve some significant population. As c increases, state 2 eventually dominates over state 1, overcoming the L' handicap, because $K_2', K_2 > K_1$. There is considerable cooperativity evident in J_a in Fig. 4 *b* because $Y = 5$ (positive cooperativity). The J_a curve from Fig. 4 *a* is included (dotted) in Fig. 4 *b* for comparison. At low c (S-1), the presence of Ca^{2+} enhances the actin-activated ATPase rate (J_a) considerably in this numerical example.

It is instructive to compare with the steady state the equilibrium binding of either MD or of an R, N mixture, using the above L' and Y values. In Eq. 11 we put either K_2' or K_2 equal to zero, respectively, and replace $3K_1c$ by K_1c or $2K_1c$, respectively. The former case corresponds to that studied in reference 1. We find for equilibrium MD binding (1) that, at $\rho = \infty$, p_2 reaches the value ½ when $c = 0.059\ \mu M$ ($\theta = 0.091$) and that $p_2 = ½$, at $\rho = 0$, when $c = 0.168\ \mu M$ ($\theta = 0.194$). These concentrations are much lower than the $p_2 = ½$ values of $c = 17\ \mu M$ ($\rho = \infty$) in Fig. 4 *a* and $c = 80\ \mu M$ ($\rho = 0$) in Fig. 4 *b*. On the other hand, for equilibrium R, N

binding (which is 150 times weaker than *MD* binding), $p_2 = \frac{1}{2}$, at $\rho = \infty$, when $c = 11.2\ \mu M$ ($\theta = 0.289$) and $p_2 = \frac{1}{2}$, at $\rho = 0$, when $c = 66.8\ \mu M$ ($\theta = 0.698$). These c values are of the same order of magnitude as in the steady-state case. This corresponds to the fact that, in the steady-state computer results at $p_2 = \frac{1}{2}$, for both $\rho = \infty$ and $\rho = 0$, the $1MD$ and $2MD$ terms in Eqs. 1 and 2, in Eq. 19, are relatively unimportant.

3. ATPASE ACTIVITY AT ARBITRARY ACTIN AND S-1 CONCENTRATIONS

In this section we combine features of the two preceding sections in order to treat steady-state ATPase activity at arbitrary actin and S-1 concentrations. Because S-1 is the enzyme molecule, we use a kinetic diagram for the states of S-1 (as in section 1), and regard actin as a ligand. But to make the model tractable, we assume that α and β (Fig. 1) are very small (as in section 2). (See also the last paragraph of section 1.) We can then use the steady-state generalization of a in section 2 to handle nearest-neighbor interactions between units without further approximation.

Each S-1 molecule in the solution behaves kinetically according to the diagram in Fig. 1 except that (*a*) α and β are very small and (*b*) A and B have to be redefined (see below) to take into account an arbitrary amount of S-1 binding on the pool of actin sites. Thus the S-1 molecules maintain a relatively "fast" steady-state distribution among the nine states in Fig. 1 (with α, β transitions omitted), against a background (or pool) of slowly changing tropomyosin-actin units (on which there is an arbitrary extent of S-1 binding) that are in quasi-equilibrium between states 1 and 2. The necessity that these two aspects of the model (fast steady state; quasi-equilibrium) have to be self-consistent requires an iteration procedure in the numerical calculations (see below).

We turn now to the details. The total concentration of S-1 is c^o and of actin (monomers) is c_A^o. Let θ_i be the fraction of state i ($i = 1, 2$) actin monomers (or sites) occupied by S-1 molecules. The total concentration of state 1 actin monomers is $(1 - p_2)c_A^o$ and the concentration of empty state 1 actin sites is $(1 - p_2)(1 - \theta_1)c_A^o$. Similarly, the concentration of empty state 2 actin sites is $p_2(1 - \theta_2)c_A^o$. These are the actin sites (free actin) available for binding to S-1. Thus, in Fig. 1, we use for A and B:

$$A = 5(1 - p_2)(1 - \theta_1)c_A^o, \quad B = 5p_2(1 - \theta_2)c_A^o. \tag{22}$$

The probabilities of the nine states in Fig. 1 ($\alpha = \beta = 0$), normalized to unity, are denoted $p_R, \ldots, p_{2MD}$. These, of course, depend on A and B. The concentration of state 1 actin sites occupied by S-1 can be expressed in two ways (in terms of actin or of S-1), and similarly for state 2. Thus we have

$$\begin{aligned}(1 - p_2)\theta_1 c_A^o &= (p_{1R} + p_{1N} + p_{1MD})c^o \\ p_2\theta_2 c_A^o &= (p_{2R} + p_{2N} + p_{2MD})c^o.\end{aligned} \tag{23}$$

The sum of these two equations gives the total concentration of actin-S-1 complexes:

$$c_A^o - c_A = c^o - c = c^o(1 - p_R - p_N - p_{MD}), \tag{24}$$

where c_A and c are the free concentrations of actin and S-1.

Each site of a state 1 unit may be in one of four states, designated 10, 1R, 1N, 1MD, with normalized probabilities (we need different notation than in the second section) $q_{10}, \ldots, q_{1MD}$. The corresponding four probabilities for a state 2 actin site are $q_{20}, \ldots, q_{2MD}$. These can be written in terms of quantities already introduced:

$$q_{i0} = 1 - \theta_i, \quad q_{iR} = \theta_i p_{iR}/(p_{iR} + p_{iN} + p_{iMD}) \qquad (i = 1, 2) \tag{25}$$

with similar expressions for q_{iN} and q_{iMD}.

From the same considerations as in the preceding section (Eqs. 12–19), we arrive again at Eq. 19 for a, with the brackets in Eq. 19 given by Eqs. 17 and 18, except that here we replace p by q and put $f = 1/2$. Eq. 10 then gives $p_2(a, Y)$.

The *a priori* parameters that enter the present problem are the numerical rate constants in Fig. 1 (with $\alpha, \beta = 0$) together with c^o, c_A^o, $L'(\rho)$, and $Y(\rho)$. Only the latter two parameters depend on Ca^{2+}. The iteration procedure we use is to: (*a*) guess initial values of p_2, θ_1, and θ_2; (*b*) calculate A and B from Eq. 22; (*c*) calculate the nine probabilities $p_R, \ldots, p_{2MD}$ in Fig. 1; (*d*) calculate the eight q's in Eq. 25; (*e*) calculate a and p_2 from Eqs. 19 and 10; and, finally, (*f*) calculate θ_1 and θ_2 from Eqs. 23. Steps (*e*) and (*f*) provide new starting values for p_2, θ_1, and θ_2. This iteration procedure is continued until convergence is obtained. However, sometimes this simple procedure diverges; more elaborate numerical methods must then be used to extend the range of convergence.

The total ATP flux per S-1 molecule is given by Eq. 8. The actin-activated ATP flux per actin monomer is (s^{-1})

$$J_a = 1{,}000(p_{1MD} + p_{2MD})c^o/c_A^o. \tag{26}$$

Numerical Calculations

To check consistency with the model in the first section ($c^o \to 0$), we have calculated $J(c_A)$ at $c^o = 0.1$ μM, with $\rho = 0$ and $\rho = \infty$, and compared these two curves with $J(c_A)$ in Fig. 2 in the case $\alpha(0) = 0.01$ s^{-1}. The results in both cases ($\rho = 0, \infty$) are indistinguishable on the scale of Fig. 2.

To compare with the second section ($c_A^o \to 0$), where actin plays the central role in the kinetic diagram, we have calculated $J_a(c)$ from the present model, at $c_A^o = 0.001$ μM, up to $c =$ 110 μM for $\rho = 0$ and up to $c = 75$ μM for $\rho = \infty$. The J_a and p_2 values are in almost exact agreement, as expected. Thus the three models have been shown to be self-consistent.

The present more general model can of course be used when the constant values of c^o and c_A^o, above, are not very small. For example, if the constant value of c^o is increased from 0.1 to 5 μM, $J(c_A)$ increases by ~10–15%, up to $c_A = 200$ μM, for both $\rho = 0$ and $\rho = \infty$.

The calculations reveal many more details than just the ATP flux, of course, but we reserve a discussion of such details for future cases that are more closely tied to experimental data.

APPENDIX

We outline here the elements of the cooperative equilibrium S-1 binding model (1) that is extended in this paper to steady-state ATPase activity.

We consider a very long actin filament saturated with troponin-tropomyosin. Each tropomyosin unit, including troponin and seven actin sites for S-1 binding, can be in one of two states: state 1, with weak binding (constant K_1) of S-1 on each of the seven actin sites; and state 2 with strong binding (constant

K_2) of S-1. The bound S-1 molecules do not interact with each other. The intrinsic equilibrium constant for $2 \rightleftharpoons 1$ in a hypothetical isolated tropomyosin unit, with no tropomyosin neighbors and with no bound S-1 or Ca^{2+}, is L, which favors state 1 (weak) over state 2 (strong) ($L > 1$). Each troponin has two equivalent binding sites for Ca^{2+} (the regulatory sites), with intrinsic binding constants K_a and K_b (in state 1 and 2, respectively). The interactions between nearest-neighbor tropomyosin molecules are of types 11, 12, 21, and 22. These boundary interactions are modulated by the extent of Ca^{2+} binding (0, 1, or 2) on the two Ca^{2+} sites of the troponin that is nearer the overlap region of the tropomyosin pair in question. We take this to be the troponin on the right-hand tropomyosin of the pair.

State 1 is favored at low S-1 concentrations ($L > 1$). But state 2 dominates at high S-1 concentrations because $K_2 \gg K_1$. The transition from state 1 to state 2 is cooperative for two reasons: because seven actin sites in a unit change state as a group; and, more importantly, because of the nearest-neighbor interactions between units.

The notation for the tropomyosin pair interactions is:

$$Y_{11} \equiv x_{11} + 2K_a\rho y_{11} + K_a^2\rho^2 z_{11}, \quad Y_{12} \equiv x_{12} + 2K_b\rho y_{12} + K_b^2\rho^2 z_{12}$$
$$Y_{21} \equiv x_{21} + 2K_a\rho y_{21} + K_a^2\rho^2 z_{21}, \quad Y_{22} \equiv x_{22} + 2K_b\rho y_{22} + K_b^2\rho^2 z_{22}, \qquad (27)$$

where ρ is the concentration of free Ca^{2+}, and x_{ij}, y_{ij}, z_{ij} are nearest-neighbor tropomyosin interaction parameters. For example, $x_{21} \equiv e^{-w_{21}/kT}$, where w_{21} is the 21 interaction-free energy with no Ca^{2+} bound on the right-hand member (in state 1) of the pair, and y_{21}, z_{21} are corresponding parameters for a 21 pair with one and two Ca^{2+} bound, respectively. Incidentally, if two bound Ca^{2+} interact with each other, this effect can be included in the z_{ij}. The Y_{ij}'s are subsystem grand partition functions (interactions and Ca^{2+} binding).

The composite parameters Y and a are defined in Eq. 4 of the main text. There is positive nearest-neighbor cooperativity if $Y > 1$ and no cooperativity of this type if $Y = 1$. The physical significance of a is mentioned following Eq. 11 of the main text.

For the equilibrium binding properties that can be deduced for this model, see reference 1.

Received for publication 2 June 1980 and in revised form 10 March 1981.

REFERENCES

1. Hill, T. L., E. Eisenberg, and L. Greene. 1980. Theoretical model for the cooperative equilibrium binding of myosin subfragment 1 to the actin-troponin-tropomyosin complex. *Proc. Natl. Acad. Sci. U.S.A.* 77:3186.
2. Greene, L., and E. Eisenberg. 1980. Cooperative binding of myosin subfragment-one to the actin-troponin-tropomyosin complex. *Proc. Natl. Acad. Sci. U.S.A.* 77:2616.
3. Bremel, R. D., J. M. Murray, and A. Weber. 1972. Manifestations of cooperative behavior in the regulated actin filament during actin-activated ATP hydrolysis in the presence of calcium. *Cold Spring Harbor Symp. Quant. Biol.* 37:267.
4. Murray, J. M., M. K. Knox, C. E. Trueblood, and A. Weber. 1980. Do tropomyosin and myosin compete for actin sites in the presence of calcium? *FEBS (Fed. Eur. Biochem. Soc.) Lett.* 114:169.
5. Trybus, K. M., and E. W. Taylor. 1980. Kinetic studies of the cooperative binding of subfragment 1 to regulated actin. *Proc. Natl. Acad. Sci. U.S.A.* 77:7209.
6. Hill, T. L., and Y. Chen. 1978. Monte Carlo calculations on critical behavior in two-state, steady-state Ising systems. *J. Chem. Phys.* 69:1126.
7. Hill, T. L., and Y. Chen. 1978. Interacting enzyme systems at steady state: further Monte Carlo calculations on two-state molecules. *Proc. Natl. Acad. Sci. U.S.A.* 75:5260.
8. Hill, T. L. 1977. Theoretical study of the effect of enzyme-enzyme interactions on steady-state enzyme kinetics. *Proc. Natl. Acad. Sci. U.S.A.* 74:3632.
9. Hill, T. L. 1977. Further study of the effect of enzyme-enzyme interactions on steady-state enzyme kinetics. *Proc. Natl. Acad. Sci. U.S.A.* 74:4111.
10. Hill, T. L. 1978. Effect of enzyme-enzyme interactions on steady-state enzyme kinetics. IV. Strictly steady-state examples. *J. Theor. Biol.* 75:391.
11. Hill, T. L. 1978. Unsymmetrical and concerted examples of the effect of enzyme-enzyme interactions on steady-state enzyme kinetics. *Proc. Natl. Acad. Sci. U.S.A.* 75:1101.

12. Hill, T. L. 1979. Steady-state phase or cooperative transitions between biochemical cycles. *Proc. Natl. Acad. Sci. U.S.A.* 76:714.
13. Hill, T. L., and L. Stein. 1980. Properties of some three-state, steady-state Ising systems according to the Bragg-Williams approximation. *Proc. Natl. Acad. Sci. U.S.A.* 77:693.
14. Hill, T. L. 1974. Theoretical formalism for the sliding filament model of contraction of striated muscle. Part I. *Prog. Biophys. Mol. Biol.* 28:267.
15. Hill, T. L. 1975. Theoretical formalism for the sliding filament model of contraction of striated muscle. Part II. *Prog. Biophys. Mol. Biol.* 29:105.
16. Hill, T. L. 1977. Free Energy Transduction in Biology. Academic Press, Inc., New York.
17. Hill, T. L., E. Eisenberg, Y. Chen, and R. J. Podolsky. 1975. Some self-consistent two-state sliding filament models of muscle contraction. *Biophys. J.* 15:335.
18. Eisenberg, E., and T. L. Hill. 1978. A cross-bridge model of muscle contraction. *Prog. Biophys. Mol. Biol.* 33:55.
19. Eisenberg, E., T. L. Hill, and Y. Chen. 1980. Cross-bridge model of muscle contraction. Quantitative analysis. *Biophys. J.* 29:195.
20. Adelstein, R. S., and E. Eisenberg. 1980. Regulation and kinetics of the actin-myosin-ATP interaction. *Annu. Rev. Biochem.* 49:921.
21. Hill, T. L. 1980. Examination of the conventional assumption of internal equilibrium within the states of a biochemical cycle. *Proc. Natl. Acad. Sci. U.S.A.* 77:205.
22. Hill, T. L. 1960. Introduction to Statistical Thermodynamics. Addison-Wesley Publishing Co., Inc., Reading, Mass.